IOP Publishing | Royal Swedish Academy of Sciences Physica Scripta

Phys. Scr. **T171** (2020) 014029 (6pp) https://doi.org/10.1088/1402-4896/ab47c7

Investigating helium–deuterium synergies in plasma-exposed tungsten using laser ablation techniques

Guin Shaw[1,4], Wendy Garcia[1], Xunxiang Hu[2] and Brian D Wirth[1,3]

[1] Nuclear Engineering Department, University of Tennessee, Knoxville, TN, United States of America
[2] Materials Science and Technology Division, Oak Ridge National Laboratory, Oak Ridge, TN, United States of America
[3] Fusion Energy Division, Oak Ridge National Laboratory, Oak Ridge, TN, United States of America

E-mail: bdwirth@utk.edu

Received 20 June 2019, revised 15 September 2019
Accepted for publication 25 September 2019
Published 2 March 2020

Abstract

This article describes the application of laser ablation based techniques to quantify the depth-dependent concentrations of gaseous species below a tungsten surface. In this work, we use a Quantel QSMART Nd:YAG 60 mJ, 5 ns frequency doubled laser that operates at a 532 nm wavelength, which we couple to an MVAT energy modulator to decrease the laser energy to 1.8 mJ. We use this laser to ablate tungsten and then characterized the resulting laser-induced plasma via laser-induced breakdown spectroscopy (LIBS). The ablated gases are pumped into a quadropole mass spectrometer to perform laser ablation mass spectroscopy (LAMS). The coupled LIBS–LAMS technique is demonstrated using a polycrystalline tungsten specimen that was helium ion implanted with variable helium ion energies to create an approximately 200 atomic parts per million flat-top concentration profile. LIBS–LAMS measurements are then performed on polycrystalline tungsten exposed to helium only, deuterium only, or 90% deuterium-10% helium plasmas on the linear plasma device PISCES/A using either a 75 or 250 eV bias voltage. The LIBS–LAMS measurements clearly indicate that exposure to helium during mixed deuterium–helium plasma exposure leads to an increased near surface deuterium concentration but reduces deuterium permeation below the tungsten surface.

Keywords: plasma surface interactions, LIBS, LAMS, helium

(Some figures may appear in colour only in the online journal)

1. Introduction

Atomistic molecular dynamics simulations of tungsten (W) indicate that hydrogen segregates to the interface of both equilibrium and high-pressure helium bubbles [1, 2], and that the de-trapping energy can range from 1.8 to 2.1 eV [2]. An appropriate question from such atomistic simulations is whether this hydrogen segregation and trapping at the surface of a high-pressure helium bubble is an artifact of the short time simulations or the interatomic potential. Experimentally, there are a number of investigations which reveal a complex helium–hydrogen interaction synergy, for which a comprehensive understanding remains lacking. For example, Ogorodnikova [3] shows that the incorporation of 10% helium in a linear plasma exposure of ITER grade tungsten substantially reduces, by approximately an order of magnitude, the amount of deterium retention in the tungsten sample relative to a pure deuterium plasma exposure. Notably, thermal desorption spectrscopy performed following mixed plasma exposure (50% 20 eV D, 33% 30 eV D, 7% 60 eV D, and 10% 60 eV He) at 320 K reveals that less deuterium desorbs in the temperature range of 400–750 K from an ITER grade W sample exposed to a 90%D–10%He plasma (again, relative to

[4] Current affiliation: Office of Fusion Energy Sciences, US Department of Energy, Office of Science, Germantown, MD United States of America.

D-only plasma exposure), but that a small D desorption peak at about 1000 K is observed in the mixed plasma exposure sample. Similarly, Doerner and co-workers report that incorporation of helium at a 5% concentration in deuterium exposures in PISCES/A substantially decreases the deuterium retention, essentially down to the detection limit by nuclear reaction analysis, for deterium exposure fluences in the range of 10^{25}–10^{28} m^{-2} at an exposure temperature of 640 K [4].

More recently, Bernard and co-workers [5] performed tritium gas loading measurements on tungsten samples exposed to a low-energy helium plasma at the PSI-2 facility. These measurements clearly indicate an increase in the tritium uptake for helium-plasma-exposed tungsten samples, although the trap binding energy was not determined. Markelj and co-authors [6] report on sequential 20 MeV tungsten self-ion irradiation followed by low-energy deuterium plasma exposure and then a 0.5 MeV helium ion implantation, in which ½ of the sample is masked from the final step of helium ion implantation. Subsequent thermal annealing and *in situ* NRA measurements confirm 'unambiguously that He attracts D and locally increases D trapping. Deuterium retention increased by a factor of two as compared to … reference … at 450 K' [6]. However, Schmid [7] notes that the deterium diffusion out of both sides of the sample occurred at the same rate indicating that 'He does not affect the solute (D) diffusion coefficient'. Thus, the experimental literature indicates the existence of trapping hydrogen at helium bubbles or a helium decorated layer, and that helium reduces the hydrogen retention, although mechanistic understanding is not yet complete. A possible explanation to reconcile these observations is that the role of a helium bubble layer within the first twenty to fifty nanometers below the surface is to locally trap deuterium, thus increasing (only) the near surface content, and also reducing deeper deuterium diffusion and permeation. An accurate depth-dependent measurement of helium and deuterium is critically important to understand the synergistic interactions of these gaseous species in tungsten.

In this article, we describe the application of laser ablation based techniques to quantify the depth-dependent concentrations of gaseous species below a tungsten surface. Section 2 describes the vacuum system established for performing laser ablation and the corresponding LIBS and LAMS measurement techniques, in addition to describing the samples and exposure conditions. Section 3 presents the results and discussion, which confirm the hypothesis that the presence of helium results in a significant increase in the near surface deuterium concentration but a decreased concentration of deuterium for depths beyond 0.1 μm following mixed deuterium–helium plasma exposure. Section 4 presents the summary.

2. LIBS–LAMS experimental technique

The LIBS–LAMS chamber was added onto an existing ultra-high vacuum chamber for performing thermal desorption spectroscopy in the low activation materials development and analysis laboratory at Oak Ridge National Laboratory, and the experimental setup will be briefly described here, with additional details provided in [8]. The Quantel QSMART Nd:YAG 60 mJ frequency doubled laser operates at a 532 nm wavelength and is coupled to an MVAT energy modulator with a pulse width of 5 ns. The energy modulator effectively lowers the laser energy without sacrificing beam quality, and through an extensive characterization, we have determined that the beam energy of 1.8 mJ can effectively produce tungsten breakdown while keeping the ablation crater depths on the order of 100 nm or less. For these laser conditions, the average crater diameter is 55 $\pm$ 15 nm, and the peak laser fluence focused onto the tungsten surface using telescoping optics is about 4.6×10^6 W cm^{-2}. The laser light is bent using a UV fused silica high power turning mirror, and then enters the vacuum chamber that contains an *X*–*Y* positioning stage through a series of collimating and translating lenses.

The sample chamber is pumped to a pressure of 5×10^{-8} Torr by a turbo, while the pressure is monitored by an MKS 909AR digital and analog hot-cathode vacuum transducers. The chamber is also coupled to the quadropole mass spectrometer, of the TDS system, through a turbo vacuum pump. Specimens are held by a standard TEM sample holder (25.4 mm diameter) on an *X*–*Y* translation stage. An optical view port for a 1 mm fiber optic provides the light from the laser ablation plasma to a Filterscope [9]. The Filterscope passes the light from the fiber optic into a series of narrow bandpass filters and then to photomultiplier tubes. The Filterscope in our LIBS–LAMS chamber can aquire high sampling rates, and contains three narrow-width bandpass filters centered at 400.52, 656.19 and 706.72 nm, respectively, to detect light emission associated with the W-I, D-alpha and He-I lines. Calibration of the LIBS signal to obtain the absolute number of W, D and He atoms is performed through the use of the S/XB coefficients assuming a constant plasma density and temperature, utilizing the FLYCHK database [10, 11], and utilizing temperature and density measurements performed by Farid and co-workers [12, 13]. More detail on the calibration of the LIBS data is provided in [8], although we believe that the largest uncertainty is due to the constant plasma and temperature assessment, and that this uncertainty is constrained by performing the complementary LAMS characterization. The impact of the assumed time independent laser-ablated plasma characteristics will be evaluated in future work.

LAMS is initiated through the vacuum turbo-pumping of the ablated gases into the QMS. The LAMS measurements used $m/q = 2$ for assessing deuterium, although we did sum the contribution from $m/q = 2$ and $m/q = 3$; and used $m/q = 4$ for helium. Multiple ablations were taken of W-only (e.g. non plasma-exposed) samples to determine the LIBS and LAMS background signals, and these background measurements were subtracted from the signal of the plasma-exposed specimen(s). The absolute quantity of He, HD, D and D_2 measured in the QMS are obtained by multiplying by a calibration constant determined through the use of a calibrated leak procedure, as described in [14] for helium calibration. Deuterium in the form of D_2 and HD captured by the

quadrupole mass spectrometer is calibrated by using a vacuum technology incorporated standard D_2 leak with a constant D_2 leak rate of 3.2×10^{-12} mol s^{-1}. A linear correlation between the mass spectrometer signal (Unit: C s^{-1}) and gas flux is assumed to calculate the calibration coefficient of D_2, and the calibration coefficient for HD and D are assumed to be the same as that of D_2. The volumetric concentration of gases in any single ablation is then obtained by dividing the absolute number of gas atoms determined from the calibrated LIBS and LAMS measurement by the ablated volume in a given laser ablation pulse, and then also corrected for the slight diametral expansion of the ablation crater with each additional laser pulse. Page limitations do not allow for a more detailed description in this article, but complete details of the crater volume analysis and correction procedure for crater expansion are provided in [8].

2.1. W samples and exposure conditions

Polycrystalline tungsten specimens, with a purity of 99.995% were procured from GoodFellow, in the form of 5 mm diameter disks that were 1 mm thick. The specimens were polished to a 0.05 μm mirrored surface finish using a colloidal silica surface polish. These specimens were then either helium ion implanted, at the University of Michigan Ion Beam Laboratory, or exposed to 75 or 250 eV biased helium, deuterium, or mixed 90%D–10%He plasmas at the PISCES/A linear plasma device at the University of California, San Diego. The helium ion implantations were sequentially performed using a variable beam energy from about 410–80 keV (in five steps, 410, 330, 220, 140 and 80 keV, respectively) at room temperature to reach an implanted helium dose of 2×10^{19} to about 6×10^{18} m^{-2}, corresponding to an approximately uniform composition of 200 atomic parts per million (appm) helium at a depth from about 0.3–0.7 μm [8].

These polycrystalline tungsten samples, along with oriented single crystal tungsten, were also exposed to either 75 or 250 eV biased plasmas, at the UCSD PISCES/A linear plasma device, with plasma ion flux values in the range of 0.7–5.4 $\times$ 10^{22} m^{-2} s^{-1}, and target surface temperatures of 300 °C and 500 °C. This article will only describe results of post-situ, vacuum LIBS–LAMS measurements of the polycrystalline tungsten samples, while the comprehensive set of results are provided in the dissertation of G Shaw [8].

3. Results and discussion

3.1. LIBS–LAMS measurements of sequential helium ion implantation to provide flat-top profile

Figure 1 presents the depth-dependent helium concentration measured using an expanding laser ablation volumetric correction to the LIBS and LAMS measurements of the polycrystalline sample exposed to sequential helium ion implantation with energies from 410 to 80 keV, resulting from averaging the data obtained from two unique laser ablation sites, each of which were subject to 15 sequential laser ablation pulses. In figure 1, the LIBS data is shown as filled blue circles, while the LAMS data is shown as filled red circles, and the SRIM predicted implanted helium concentration as a function of depth is shown as the solid line. Figure 1 also includes elastic recoil detection analysis results on this sample as filled yellow squares, which were performed by K Woller (MIT). In the interest of brevity, this article does not present the results of several different analysis to assess the degree of uncertainty due to the assumption of constant laser ablation plasma temperature and density or the crater volume and shape, although those results are presented in detail in [8]. The lateral error bars in figure 1, result from the uncertainty of the spatial mid-point of the laser ablated crater with each subsequent laser ablation, while the vertical error bars represent the known uncertainties in assessing the crater volume and calibration of LIBS and LAMS, respectively, averaged over the two unique laser ablation locations. Overall, the results of figure 1 clearly demonstrate that the combined use of LIBS and LAMS can resolve the depth-dependent concentration of helium, and that the measured concentrations are in quite good agreement with the SRIM predicted implantation profile. Further, the LIBS and LAMS measurements are in good agreement with each other, within our known uncertainty. As noted in section 2, the key uncertainties in these measurements relate to assessing the ablated volume, the correction for crater width expansion, and the assumption that the S/XB coefficients are not time varying. Subsequently, when presenting the results of LIBS–LAMS measurements of samples exposed to low-energy plasmas, we will average the LIBS and LAMS measurements together, to further reduce the uncertainty associated with each individual technique. One other factor that must be considered is the impact of the heat affected zone surrounding the ablation crater. The good agreement shown in figure 1 provides confidence that this does not substantially impact

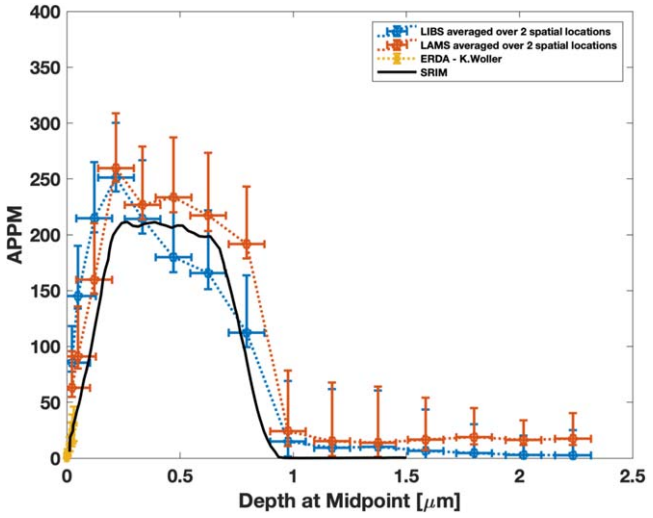

Figure 1. Depth-dependent LIBS (blue circle) and LAMS (red circle) measurement of helium concentration in tungsten following sequential ion implantation, as compared to the SRIM prediction of implanted concentration (line) and ERDA measurements (yellow square) performed by K Woller (MIT).

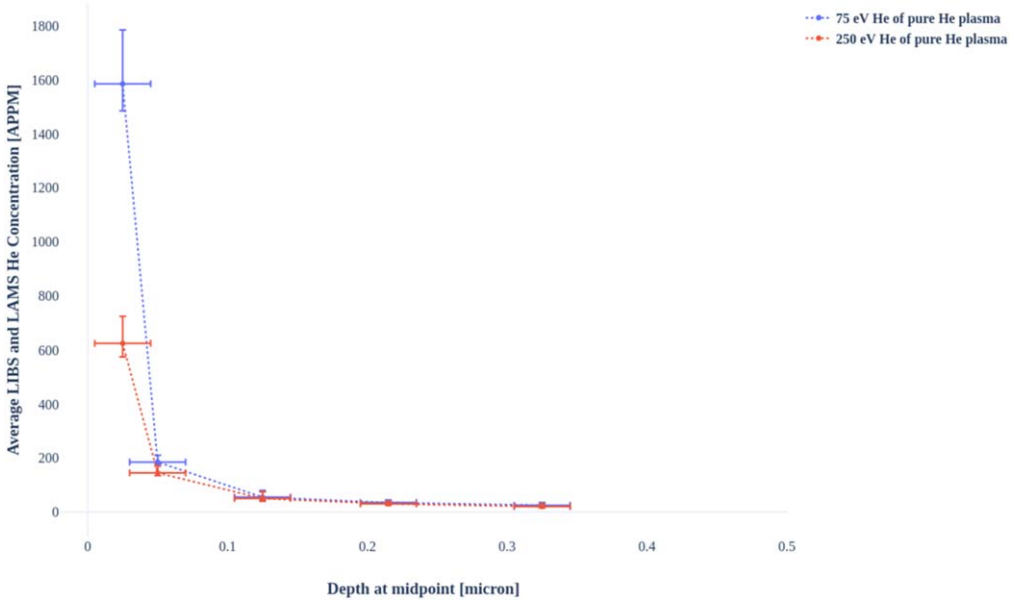

Figure 2. Depth-dependent LIBS–LAMS (note LIBS and LAMS results averaged) of 75 (blue) or 250 eV (red) helium plasma-exposed polycrystalline tungsten.

helium desorption, although it may lead to additional deuterium release as noted in section 3.2.

3.2. LIBS–LAMS measurements of low-energy plasma-exposed W

Figure 2 presents the LIBS–LAMS measurements of depth-dependent He concentration from the helium plasma-exposed polycrystalline tungsten at an initial target temperature of 500 °C to a helium fluence of about 3×10^{24} (250 eV, red circles) to about 1.2×10^{26} (75 eV, blue circles) m^{-2}. In figure 2, the LIBS and LAMS volume corrected data has been averaged to obtain a single data point, based on the good agreement presented in figure 1. The results shown in figure 2 clearly indicate that helium is localized in the near surface region, with a higher local helium concentration measured following the 75 eV versus 250 eV helium plasma exposure. The reason for the higher surface concentration following 75 eV helium plasma exposure is multiple, first the sample exposed to the lower energy plasma was exposed for a longer time (4000 s) compared to the 250 eV plasma (∼150 s), and secondly, the 250 eV bias voltage implants helium ions with energies above the sputtering threshold resulting in surface erosion. These two effects are consistent with the lower helium concentration of approximately 600 appm measured in the sample exposed to 250 eV helium plasma compared to the 75 eV plasma (approximately 1600 appm) in the very near surface region. Notably, the measured helium content drops to nearly zero beginning with the 3rd laser ablation (at depths beyond about 120 nm), which demonstrates a very different depth-dependent helium population than for the sequential ion implantation results shown in figure 1, and the helium concentrations plotted in figure 2 are generally consistent with TEM measurements of Miyamoto and co-workers [15] and glancing incident small angle x-ray scattering [16], both of which show a layer of helium bubbles at a depth of about 20 nm below tungsten surfaces.

Figure 3 presents the the LIBS–LAMS measurements of the depth-dependent helium (figure 3(a)) and deuterium (figure 3(b)) concentration for polycrystalline tungsten samples exposed to either a pure deuterium or mixed 90%D–10%He plasma with an applied bias voltage of 75 eV and an initial sample temperature of 500 °C. Figure 3(a) indicates that a very small concentration of helium is measured following pure D plasma exposure, which may result from impurity helium in the plasma and PISCES chamber, or indicate some quantity of D_2 measured in the QMS during LAMS, although the values are quite small, on the order of 20 appm. The quantity of helium measured following mixed plasma exposure is on the order of 250 appm, which is much less than following helium plasma exposure (figure 2), but again a much higher helium concentration is observed within the first two to three ablations (∼100–150 nm below the surface). Thus, the helium concentration demonstrates a similar depth dependence to the helium only plasma exposure measurement shown in figure 2. Figure 3(b) shows the measured D concentration as a function of depth.

It is important to note that the heat affected zone surrounding the laser ablation crater is much more likely to release deuterium (than helium), and thus we have additional uncertainty in correcting the near surface deuterium concencentration measured in the first few laser ablations. However, a robust conclusion can be drawn by comparing the deuterium profile following deuterium only versus mixed 90%D–10%He plasma exposure; namely it is evident that deuterium is detected at much deeper depths following D-only plasma exposure than following mixed D–He plasma exposure. As well, the near surface concentration of D is much higher following mixed D–He plasma exposure. Thus, we conclude that the presence of He results in a near surface increase in deuterium concentration, but a decrease in the deeper diffusion (permeation) of deuterium. This result is

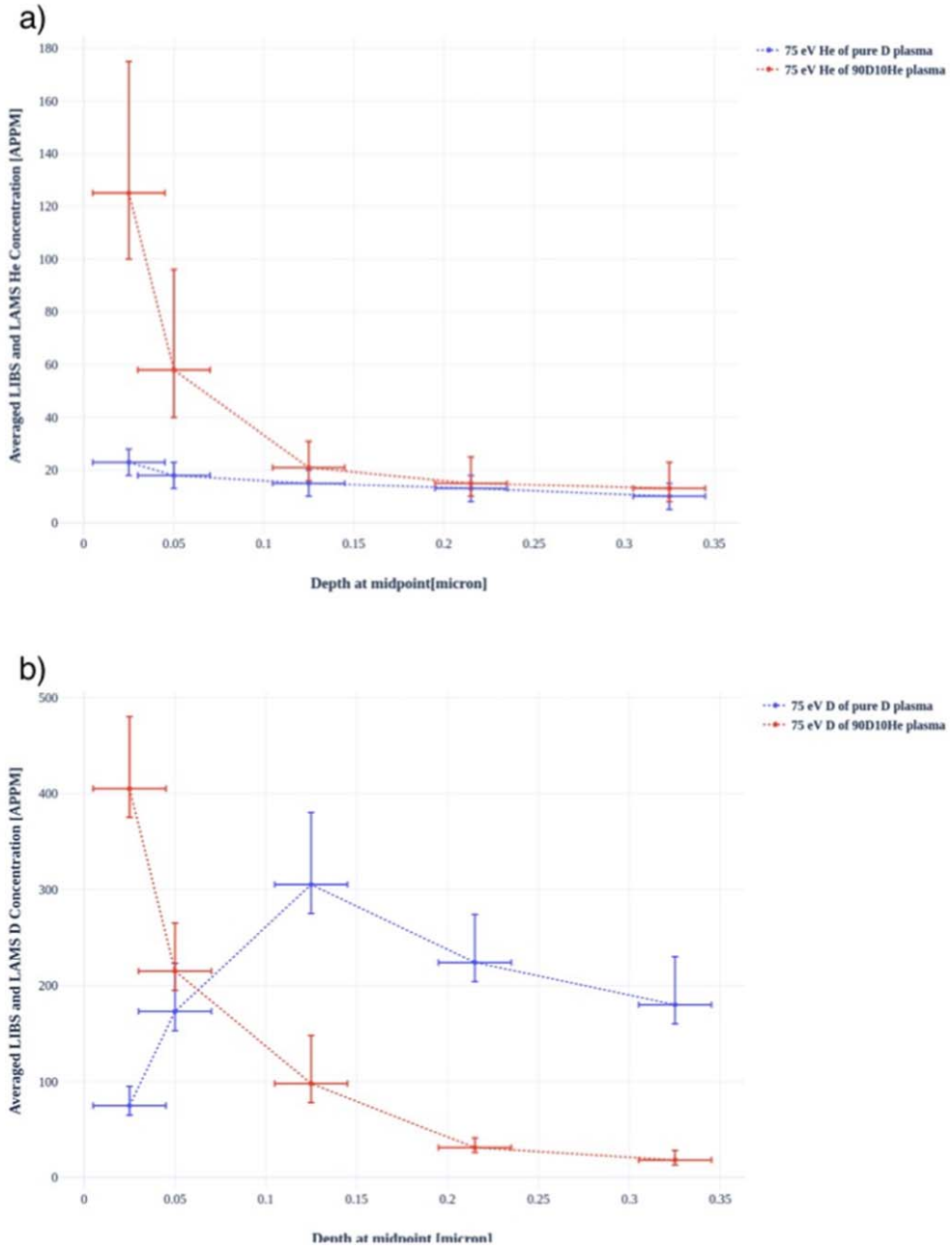

Figure 3. Depth-dependent LIBS–LAMS (note LIBS and LAMS results averaged) measurements of (a) helium and (b) deuterium, following 75 eV plasma-exposed polycrystalline tungsten to either a pure D (filled blue circles) or 90%D–10%He (filled red circles) plasma.

consistent with the measurements of Markelj and co-workers [6] as well as the role of helium in deuterium trapping and permeation discussed previously.

Figure 4 presents the LIBS–LAMS measurements of depth-dependent D concentration from the helium plasma-exposed polycrystalline tungsten and an initial target temperature of 500 °C, and compares the bias voltage of 75 eV versus 250 eV. The difference between the sub-surface D concentrations following 75 versus 250 eV plasma exposure are minimal, and within the experimental error, and again, the largest differences in deuterium behavior are observed for mixed 90%D–10%He compare to pure D plasma exposure. The conclusion regarding the effect of helium on deuterium concentration below the surface remains the same, namely that there is a clear increase in the very near surface concentration of deuterium following mixed D–He plasma exposure, relative to D-only plasma exposure. And, there is a significant decrease in the amount of deuterium at deeper depths (beyond 120 nm) following mixed D–He plasma exposure at both 75 and 250 eV compared to the D-only plasma exposure.

4. Summary and future work

This article presents results documenting the development of a laser based ablation technique, which combines the measurement

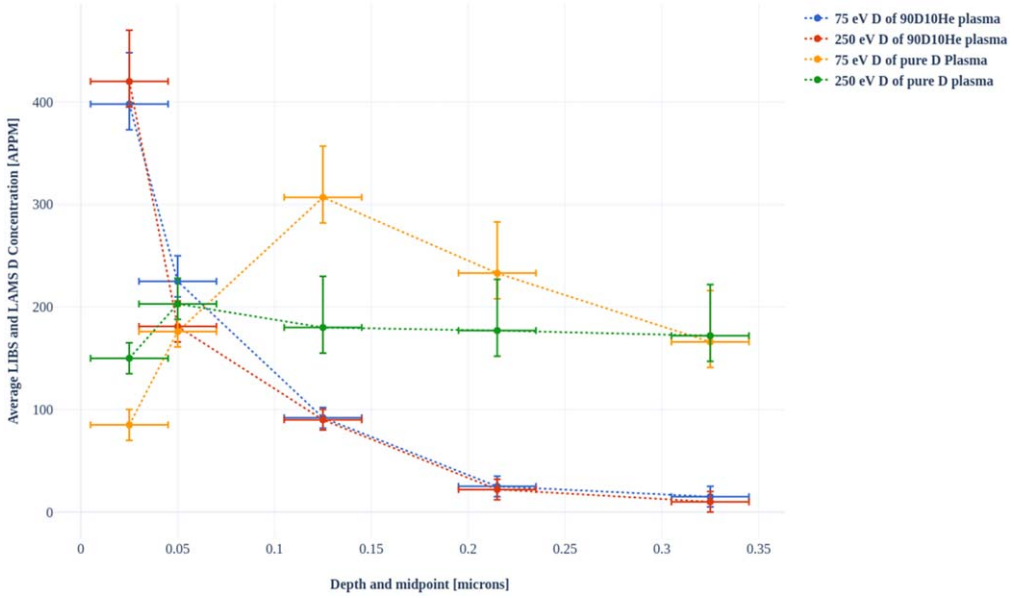

Figure 4. Depth-dependent LIBS–LAMS (note LIBS and LAMS results averaged) measurements of D concentration following either 75 eV or 250 eV plasma-exposed polycrystalline tungsten to either a pure D (filled yellow or green circles for 75/250 eV) or 90%D–10%He (filled blue or red circles for 75/250 eV) plasma.

of laser-induced breakdown spectroscopy with laser ablation mass spectrometry, to measure the depth-dependent gas concentrations in fusion plasma facing components. We demonstrate this technique by measuring the depth dependence of helium that was ion implanted with a sequential set of ion energies to produce a nearly flat-top helium concentration at about 200 appm for depths between 0.3 and 0.7 microns, and the measured concentrations agree well with SRIM simulations of the implantation profile. Subsequently, we apply the coupled LIBS–LAMS technique to measure polycrystalline tungsten exposed to helium only, deuterium only, or 90% deuterium-10% helium plasmas on the linear plasma device PISCES/A using either a 75 or 250 eV bias voltage. The LIBS–LAMS measurements clearly indicate that exposure to helium during mixed deuterium–helium plasma exposure leads to an increased near surface deuterium concentration but reduced deuterium permeation below the tungsten surface.

Acknowledgments

We gratefully acknowledge the contributions of Dr Russ Doerner (UCSD) for the PISCES/A plasma exposure of the polycrystalline tungsten specimens used in this work, and to Dr Kevin Woller (MIT) for performing the ERDA measurement on the helium ion implanted tungsten sample. Financial support was provided by the DOE Office of Fusion Energy Sciences (FES) through award DE-SC0006661 at UTK. XH acknowledges FES support under Grant No. DE-AC05-00OR22725 with UT-Battelle LLC, and the use of the PISCES/A facility was supported by DOE FES Grant No. DE-FG02-07ER54912.

ORCID iDs

Brian D Wirth https://orcid.org/0000-0002-0395-0285

References

[1] Juslin N and Wirth B D 2011 *J. Nucl. Mater.* **438** 1221
[2] Bergstrom Z, Cusentino M A C and Wirth B D 2017 *Fusion Sci. Technol.* **71** 122
[3] Ogorodnikova O, Schwarz-Selinger T, Sugiyama K and Alimov V 2011 *J. Appl. Phys.* **109** 013309
[4] Doerner R P, Baldwin M J, Lynch T C and Yu J H 2016 *Nucl. Mater. Energy* **9** 89
[5] Bernard E *et al* 2017 *Phys. Scr.* **T170** 014023
[6] Markelj S, Schwarz-Selinger T and Zaloznik A 2017 *Nucl. Fusion* **57** 064002
[7] Schmid K *et al* 2017 *Phys. Scr.* **T170** 014037
[8] Shaw G 2019 Quantification of hydrogen–helium retention in tungsten using laser induced breakdown spectroscopy coupled with laser ablation mass spectrometry *PhD Thesis* University of Tennessee, Knoxville
[9] Colchin R J, Hillis D L, Maingi R, Klpeer C C and Brooks N H 2003 *Rev. Sci. Instrum.* **74** 2068
[10] Chung H-K, Chen M, Morgan W, Ralchenko Y and Lee R 2005 *High Energy Density Phys.* **1** 3
[11] Janev R K, Langer W D, Evans, Jr. K and Post, Jr. D E 2012 *Elementary Processes in Hydrogen-Helium Plasmas: Cross Sections and Reaction Rate Coefficient* (*Springer Series on Atoms and Plasmas*) ed *et al* vol 4 (Berlin: Springer-Verlag) Springer Science & Business Media **4**
[12] Farid N, Harilal S S, Ding H and Hassanein A 2014 *J. Appl. Phys.* **115** 033107
[13] Farid N, Li C, Wang H and Ding H 2013 *J. Nucl. Mater.* **433** 80
[14] Hu X, Field K G, Taller S, Katoh Y and Wirth B D 2017 *J. Nucl. Mater.* **489** 109
[15] Miyamoto M *et al* 2011 *J. Nucl. Mater.* **415** S657
[16] Thompson M *et al* 2015 *Nucl. Fusion* **55** 42001